Engineering Notes

Modeling the Vertical Motion of a Zero Pressure Gas Balloon

J.-L. Robyr,* V. Bourquin,† D. Goetschi,‡ N. Schroeter,§ and R. Baltensperger¶
University of Applied Sciences and Arts Western Switzerland, CH-1700 Fribourg, Switzerland

https://doi.org/10.2514/1.C035890

Downloaded by Karina Bustillo on September 25, 2020 | http://arc.aiaa.org | DOI: 10.2514/1.C035890

Nomenclature

A_{top}	=	cross-sectional area of a sphere with volume equivalent to the balloon, m^2
C_D	=	drag coefficient; 0.5
c_f	=	specific heat of the balloon film; 2302.7 $J \cdot kg^{-1} \cdot K^{-1}$
c_{pg}	=	specific heat of the balloon lifting gas (hydrogen); 14,320.0 $J \cdot kg^{-1} \cdot K^{-1}$
g	=	Earth gravitational acceleration; 9.81 $m \cdot s^{-2}$
M_a	=	molecular weight of air; 28.96 $kg \cdot kmol^{-1}$
M_g	=	molecular weight of the gas (hydrogen); 2.02 $kg \cdot kmol^{-1}$
m_f	=	mass of the balloon film; 100 kg
m_g	=	mass of the balloon gas, kg
m_{tot}	=	total mass of the system, kg
m_v	=	virtual mass, kg
$\dot{q}_f$	=	net heat flux to the balloon film, W
$\dot{q}_g$	=	net heat flux to the balloon gas, W
T_f	=	balloon film temperature, K
T_g	=	balloon gas temperature, K
t	=	time, s
V	=	volume of gas, m^3
z	=	altitude of balloon, m
ρ_a	=	density of air, $kg \cdot m^{-3}$

I. Introduction

THE existing literature on gas balloon motion can be split into precise computing of the balloon trajectory in wind fields with weather model data and the study of the balloon vertical motion due to the heat exchange with its direct environment. The combination of these two fields allows us to simulate real balloon flights. The reference works for both approaches are the ones of Kreith and Kreider [1], Morris [2], and Carlson and Horn [3].

The balloon trajectory studies are mainly used for high-altitude gas balloons to avoid, for example, collision accidents or predict their landing region. Palumbo et al. in Ref. [4], Sóbester et al. in Ref. [5], and Lee and Yee in Ref. [6] used Monte Carlo techniques to predict the trajectory of a high-altitude gas balloon. Renegar in Ref. [7] made a recent survey of the present state of available balloon trajectory prediction systems. In a more controlled manner, Aaron et al. in Ref. [8] and, more recently, Waghela et al. proposed in Ref. [9] trajectory control systems capable of guiding a high-altitude balloon.

Few works were dedicated to the study of manned gas balloon flights. The only works we found on this subject were the one of Das et al. in Ref. [10], Furfaro et al. in Ref. [11], Baumann and Stohl in Ref. [12], and Ellenrieder in Ref. [13].

The principal physics laws determining gas balloon trajectories have been extensively studied in the literature. The heat exchange between the balloon's elements (envelope, gas, etc.) and its surroundings is essential. For example, Dai et al. in Ref. [14] tried to characterize the influence of film radiation properties and clouds on balloon thermal behaviors in order to operate safe and reliable high-altitude balloons. For a review on those works, see the work of Yajima et al. [15] for example.

The present work focuses on a manned balloon filled with hydrogen flying below 6000 m. Our main source is the work of Saleh and He [16], which is adapted from Ref. [3]. We will compare our model to real data and try to simulate part of two recorded manned gas balloon flights. Our data come from two races (2016 Gordon Bennett cup** and 2017 America's Challenge††) done by the Fribourg Freiburg Challenge Swiss team (FR-CHallenge)‡‡. We propose an analysis and adaptation of our primary model in order to reproduce the complex ascension dynamics of real flights.

II. Mathematical Model

We follow the development proposed in Ref. [16] to derive the thermal and dynamical model of a zero pressure gas balloon based on Ref. [3] with a variable amount of direct and reflected solar radiation.

Based on the thermal and dynamical model of gas balloons proposed in Ref. [3] and used in Refs. [10,15], the vertical motion of a zero pressure gas balloon can be described by the vertical force-balance equation

$$(m_{\text{tot}} + m_v) \cdot \frac{\mathrm{d}^2 z}{\mathrm{d}t^2} = g \cdot (\rho_a \cdot V - m_{\text{tot}}) - \frac{1}{2} \cdot \rho_a \cdot A_{\text{top}} \cdot C_D \cdot \frac{\mathrm{d}z}{\mathrm{d}t} \cdot \left| \frac{\mathrm{d}z}{\mathrm{d}t} \right| \tag{1}$$

where $z = z(t)$ represents the vertical position (in meters) of the (zero pressure) gas balloon at time t.

The heat-balance equations for the balloon film and lifting gas are taken from Refs. [3,10,16] and read

$$m_f \cdot c_f \cdot \frac{\mathrm{d}T_f}{\mathrm{d}t} = \dot{q}_f \tag{2}$$

$$m_g \cdot c_{pg} \cdot \frac{\mathrm{d}T_g}{\mathrm{d}t} = \dot{q}_g - \left(\frac{g \cdot M_a \cdot m_g \cdot T_g}{T_a \cdot M_g} \right) \cdot \frac{\mathrm{d}z}{\mathrm{d}t} \tag{3}$$

The heat flux of the film $\dot{q}_f$ and of the gas $\dot{q}_g$ in Eqs. (2) and (3) can be found, for example, in Ref. [3].

Received 14 February 2020; revision received 7 April 2020; accepted for publication 14 May 2020; published online 2 June 2020. Copyright © 2020 by the American Institute of Aeronautics and Astronautics, Inc. All rights reserved. All requests for copying and permission to reprint should be submitted to CCC at www.copyright.com; employ the eISSN 1533-3868 to initiate your request. See also AIAA Rights and Permissions www.aiaa.org/randp.

*Research Associate, Department of Mechanics and Physics, School of Engineering and Architecture Fribourg, Bd de Pérolles 80.
†Professor, Department of Mechanics, School of Engineering and Architecture Fribourg, Bd de Pérolles 80.
‡Research Associate, Department of Computer Science, School of Engineering and Architecture Fribourg, Bd de Pérolles 80.
§Professor, Department of Computer Science, School of Engineering and Architecture Fribourg, Bd de Pérolles 80.
¶Professor, Department of Mathematics and Physics, School of Engineering and Architecture Fribourg, Bd de Pérolles 80.

**Bennett, G., "Gordon Bennett Cup (Ballooning)," 1906.
††"America's Challenge," 1995, https://balloonfiesta.com/Americas-Challenge.
‡‡"FRIBOURG FREIBURG CHALLENGE," 2015, http://frchallenge.ch/.

Downloaded by Karina Bustillo on September 25, 2020 | http://arc.aiaa.org | DOI: 10.2514/1.C035890

III. Simulation

We analyze and simulate a portion of the flight where the balloon was flying freely with no active altitude change made by the pilots (gas exhaust or ballast drop). The first flight occurred during the America's challenge race (see footnote ††) in 2017, where the FR-CHallenge team established a new world record of a distance of more than 3600 km in a competition. The second race is the 2016 Gordon Bennett cup (see footnote **), where the team reached the second place.

To isolate the change of altitude due to the heat exchange only, we have selected flight data during the transition between night and day.

In order to validate the choice of the physical parameters for the simulation of the FR-CHallenge balloon, we first have performed comparison and adaptation on the model based on the America's Challenge flight of 2017. Finally, we have applied exactly the same model to the Gordon Bennett flight of 2016 with a simple linear scaling.

For both flights, the same white coated balloon envelope has been used. The radiative properties of the envelope have been modelled by a film with an absorptivity of 0.20, a reflectivity of 0.80, an emissivity of 0.9, and no transmissivity.

The international standard atmosphere (ISA) is used in the simulation.

A. America's Challenge Flight of 2017

In the America's Challenge flight, the FR-CHallenge team flew from Albuquerque in the United States to Labrador City in Canada. The data of the vertical motion of the balloon are presented in Fig. 1, with the analyzed section in red.

The simulation begins shortly before sunrise on the second day of the race (on 9 October 2017 at 12:10 coordinated universal time (UTC)). The altitude of the balloon at that time was around 3200 m above see level (ASL). This point almost corresponds to the third vertical line in Fig. 1.

At this moment of the race, the hydrogen gas does not completely fill the balloon envelope. This phenomenon is due to the vertical pressure gradient in the atmosphere, which has the consequence that the gas fully fills the balloon envelope only at a higher altitude where the pressure corresponds to proper thermodynamic conditions for the gas to fully fill the envelope, refered as altitude of plenitude. Below this highest point, the balloon envelope is partially filled, making it lose its spherical shape. For this flight, the envelope plenitude was at 4800 m ASL. We have set the sand ballast to 326 kg according the race data, and the balloon is started at rest.

Although the pilots did not do any maneuver, we can see that the balloon is rising in three elevation phases (see the blue curve in Fig. 2). A first rapid ascension (in Fig. 2, section a between the two first vertical lines), a moderate second phase (in Fig. 2, section b), and a slow third phase (in Fig. 2, section c) before reaching an altitude of envelope plenitude at around 4800 m ASL.

We know that, for reaching a final stabilized altitude with an envelope plenitude of 4800 m, we need to have a ballast sand mass of 326 kg. If we simulate the balloon ascent with this initial condition, the balloon reaches 4800 m in about half an hour (see Fig. 2, green curve), which is much faster than the observed flight, except for the beginning of the ascending phase (section a in Fig. 2). If one increases the ballast mass by 77 kg, the altitude of the envelope plenitude is lowered and the ascension is stopped at around 3800 m (see Fig. 3, green curve).

To make the balloon rise to 4800 m without active control from the pilots, one needs to find a two-phase natural loss of ballast. This mechanism can be explained by the condensation of water on the balloon film during the night that drops from the balloon envelope and evaporates once the sun rises. This additional water changes the total ballast for some time. This phenomenon has been confirmed by the pilots, although it is not possible to evaluate the quantity of water condensed on the balloon envelope. The water loss occurs in two steps, as simulated in Figs. 4 and 5.

The first rapid rising phase (section a in Fig. 4) lasts 30 min and begins just after sunrise. The lifting gas is heated by the sun, and the balloon rises quickly to an altitude of around 3800 m ASL. During this phase, there is no ballast drop. The second moderate phase (section b in Fig. 4, green curve) lasts 65 min with a constant water

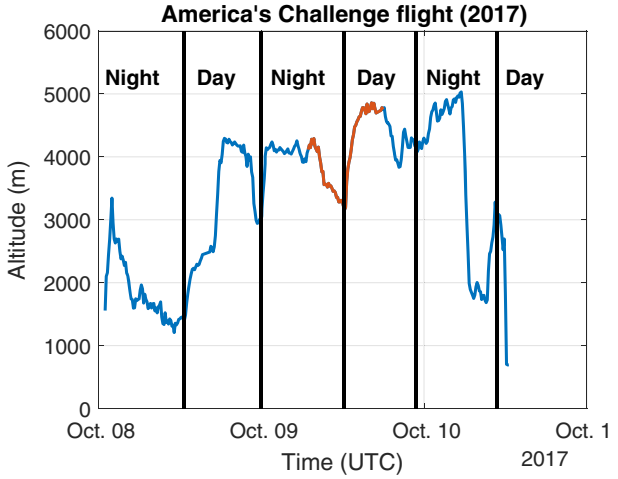

Fig. 1 Altitude data from the FR-CHallenge's 2017 winning flight from Albuquerque to Labrador City (blue curve) and the analyzed portion (red curve).

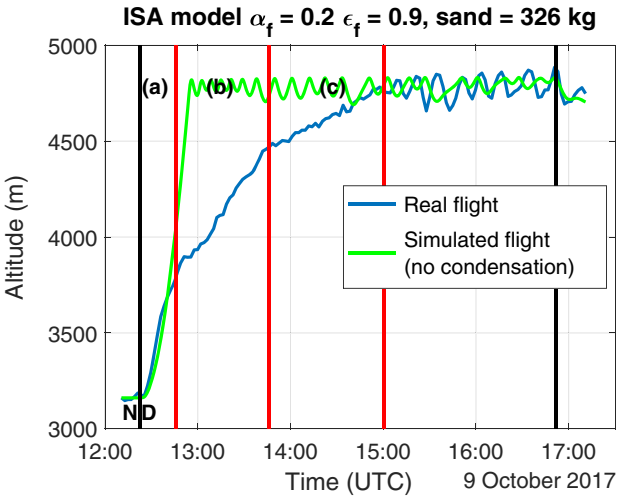

Fig. 2 Simulation of America's Challenge flight (2017) balloon rise due to sunrise with no water condensation. N (resp. D) refers to night (resp. day).

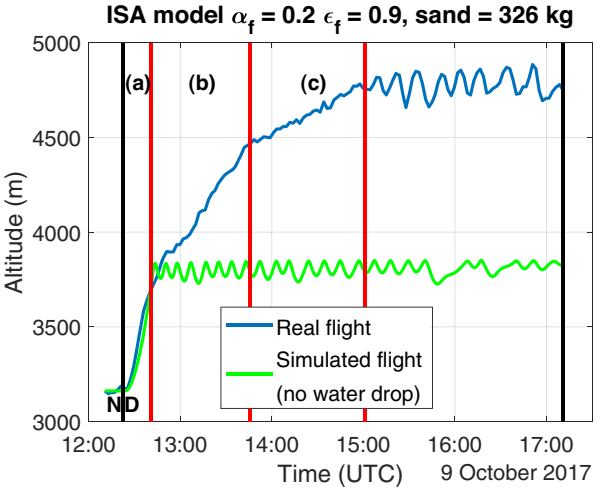

Fig. 3 Simulation of America's Challenge flight (2017) balloon rise due to sunrise with additional water ballast (77 kg) but no water drop.

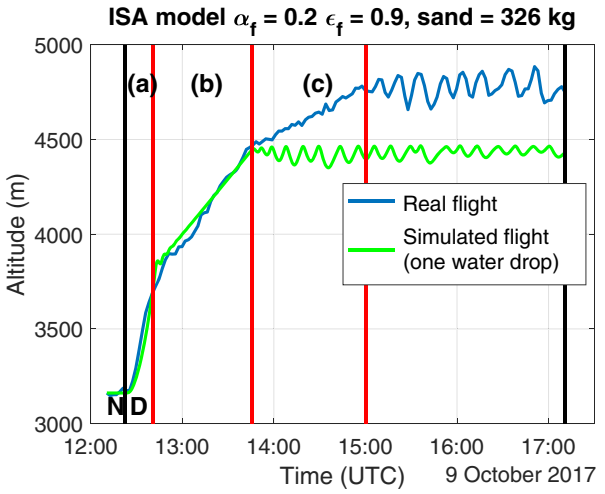

Fig. 4 Simulation of America's Challenge flight (2017) balloon rise due to sunrise: simulation of the flight with additional water of 77 kg and one water drop of 49 kg in phase (section b).

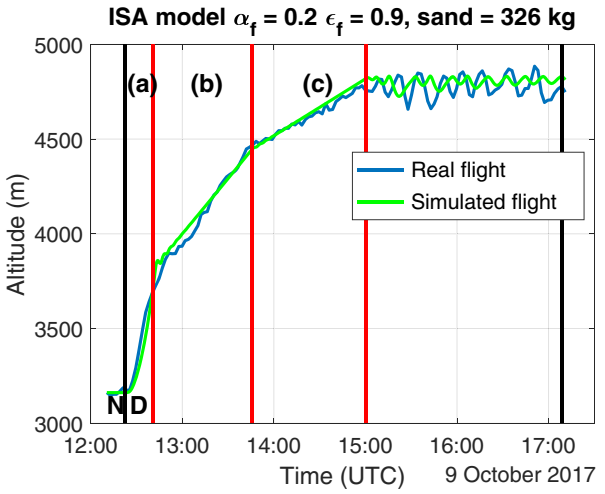

Fig. 5 Simulation of flight with water condensation. Ascension of balloon modeled by three distinct phases: only sun heating (section a), constant water drop rate totalling 49 kg (section b), and continuous ballast drop of 28 kg (section c).

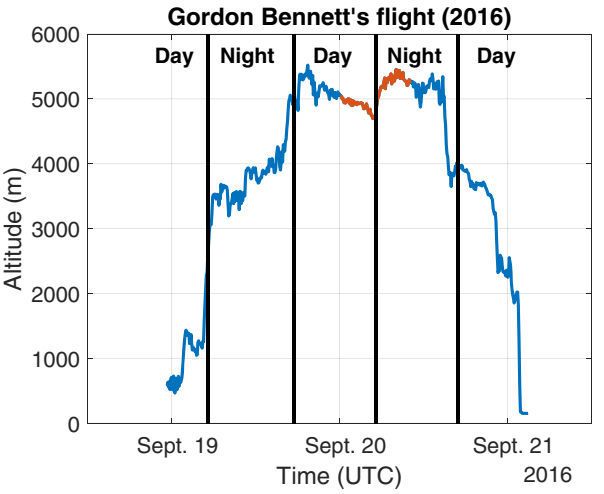

Fig. 6 Altitude of the FR-CHallenge's flight (Gordon Bennett 2016) from Gladbeck (Germany) to south of Italy (blue curve) with the analyzed portion (red curve).

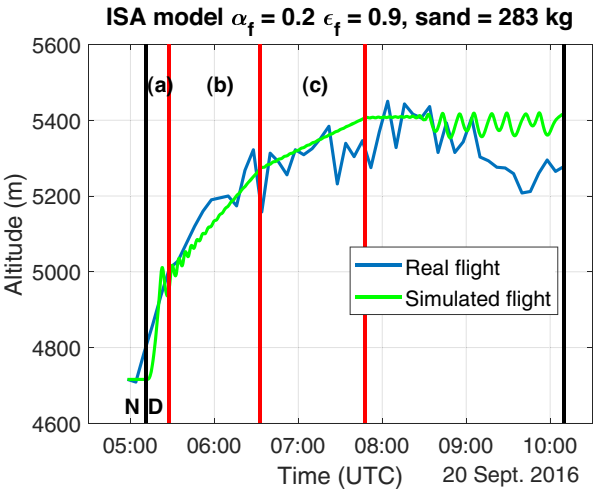

Fig. 7 Simulation of Gordon Bennett flight (2016) with sunrise effect. The three rising phases are the sun only for 30 min (section a), water drop of 19 kg for 65 min (section b), and water drop of 9 kg for 75 min (section c).

drop rate totalling 49 kg. This water drop is probably due to the accumulated dew on the balloon envelope during the night that falls due to gravity. This water drop causes the slow ascending phase.

The third (slow) phase (section c in Fig. 5, green curve) lasts 75 min with a constant water drop rate totalling 28 kg. We guess that this water drop is due to evaporation or could represent the rest of the water flow, and it slows down the final ascending velocity of the balloon.

After these three ascending phases, the balloon stabilizes at an altitude of around 4800 m ASL with some oscillations (as the one observed in the real flight). The last black vertical line (in Fig. 2) represents the time when the solar radiation is at its peak. After this time in the simulation, the balloon will fall due to cooling of the hydrogen from the decrease of the sun power.

B. Gordon Bennett Flight of 2016

We also simulated the flight of FR-CHallenge during the Gordon Bennett race of 2016. The race began in Gladbeck (Germany) on 19 September 2016 and ended in the south of Italy.

The studied sunrise-triggered ascension of the balloon occurs at the end of the second night (20 September 2016 at 04:57:53 UTC) at around 4710 m ASL, as shown in red in Fig. 6. The balloon is set at rest with a (sand) ballast of 283 kg (corresponding to an altitude of plenitude of around 5400 m ASL).

Similarly to the America's Challenge, the pilots did not do any maneuver during this period, and the balloon is rising in three elevation phases (see the blue curve in Fig. 7). A rapid first phase (section a in Fig. 7), a moderate second phase (section b in Fig. 7), and a slow third phase (section c in Fig. 7) before reaching an altitude of plenitude of the balloon envelope at around 5400 m ASL.

Like in Sec. III.A, the three decreasing ascension velocities are obtained by increasing the total ballast for this flight by 28 kg of water. Otherwise, the balloon would have risen up to its altitude of plenitude (at around 5400 m ASL) in less than 1 h, which is obviously not the case. The durations of these phases are the same as in the America's Challenge race, respectively, 30 min (section a in Fig. 7), 65 min (section b in Fig. 7), and 75 min (section c in Fig. 7). The correspondence of the three-phase duration between the two flights suggests that the phenomenon causing it is the same. After these three ascending phases, the balloon stabilizes at an altitude of (around) 5400 m ASL with some oscillations (like in the real flight). The last black vertical line represents the end of the simulation.

IV. Conclusions

A model to predict the vertical motion of a zero pressure manned gas balloon at sunrise was proposed. The work was based on existing works on high-altitude gas balloon physical models.

Downloaded by Karina Bustillo on September 25, 2020 | http://arc.aiaa.org | DOI: 10.2514/1.C035890

An attempt was made to simulate chosen parts of real flights (Gordon Bennett flight of 2016 and America's Challenge flight of 2017 of the FR-CHallenge team) with a high level of accuracy at sunrise. The balloon is white coated and evolved in a standard atmosphere. To reproduce the balloon trajectories that show three distinct ascending phases, additional ballast interpreted as condensed water accumulating during the night on the balloon film was implemented. The first rapid ascending phase lasts around 30 min while the balloon reaches its maximal volume corresponding to its envelope plenitude. The second phase lasts around 60 min and occurs when the water drops from the envelope due to gravity. The third phase lasts about 75 min. It occurs when the remaining water drops or evaporates. This additional ballast water drop explains very well the progressive slowing in the ascending phases of the balloon. The three ascending phases have similar durations in the two simulated flights, although the altitudes and atmospheric conditions were different: a fact that strengthens the proposed model.

Acknowledgments

The authors gratefully acknowledge the support provided by the institutes Sustainable Engineering Systems Institute, the Institute of Smart and Secured Systems, the Technology for Human Wellbeing Institute, and the directorate of the School of Engineering and Architecture of Fribourg in conducting this research. We would like to thank the Fribourg Freiburg Challenge team for being open to and ready for discussions at any time on the present work. We would like to thank Frédéric Bapst and Micha Wasem for helpful comments on drafts of the present Note. We would like to especially thank our colleague Aleš Janka for stimulating discussion while we were working on the present Note.

References

[1] Kreith, F., and Kreider, J. F., "Numerical Prediction of the Performance of High Altitude Balloons," National Center for Atmospheric Research (NCAR) NCAR-IN/STR-65, 1974. https://doi.org/10.5065/D64X55SR

[2] Morris, A., "Scientific Ballooning Handbook," NCAR TN/1A-99, 1975. https://doi.org/10.5065/D6G73BM1

[3] Carlson, L. A., and Horn, W. J., "New Thermal and Trajectory Model for High-Altitude Balloons," *Journal of Aircraft*, Vol. 20, No. 6, 1983, pp. 500–507. https://doi.org/10.2514/3.44900

[4] Palumbo, R., Morani, G., and Corraro, F., "Effective Approach to Characterization of Prediction Errors for Balloon Ascent Trajectories," *Journal of Aircraft*, Vol. 47, No. 4, 2010, pp. 1331–1337. https://doi.org/10.2514/1.47005

[5] Sóbester, A., Czerski, H., Zapponi, N., and Castro, I., "High-Altitude Gas Balloon Trajectory Prediction: A Monte Carlo Model," *AIAA Journal*, Vol. 52, No. 4, 2014, pp. 832–842. https://doi.org/10.2514/1.J052900

[6] Lee, Y., and Yee, K., "Numerical Prediction of Scientific Balloon Trajectories While Considering Various Uncertainties," *Journal of Aircraft*, Vol. 54, No. 2, 2017, pp. 768–782. https://doi.org/10.2514/1.C033998

[7] Renegar, L. W., "A Survey of Current Balloon Trajectory Prediction Technology," *Academic High-Altitude Conference*, Stratospheric Ballooning Assoc. (unpublished).

[8] Aaron, K., Heun, M., and Nock, K., "Balloon Trajectory Control," AIAA Paper 1999-3865, 1999. https://doi.org/10.2514/6.1999-3865

[9] Waghela, R., Yoder, C. D., Gopalarathnam, A., and Mazzoleni, A. P., "Aerodynamic Sails for Passive Guidance of High-Altitude Balloons: Static-Stability and Equilibrium Performance," *Journal of Aircraft*, Vol. 56, No. 5, 2019, pp. 1849–1857. https://doi.org/10.2514/1.C035353

[10] Das, T., Mukherjee, R., and Cameron, J., "Optimal Trajectory Planning for Hot-Air Balloons in Linear Wind Fields," *Journal of Guidance, Control, and Dynamics*, Vol. 26, No. 3, 2003, pp. 416–424. https://doi.org/10.2514/2.5079

[11] Furfaro, R., Lunine, J. I., Elfes, A., and Reh, K., "Wind-Based Navigation of a Hot-Air Balloon on Titan: A Feasibility Study," *Space Exploration Technologies*, Vol. 6960, edited by W. Fink, International Soc. for Optics and Photonics, SPIE, Bellingham, WA, 2008, pp. 92–104. https://doi.org/10.1117/12.777654

[12] Baumann, K., and Stohl, A., "Validation of a Long-Range Trajectory Model Using Gas Balloon Tracks from the Gordon Bennett Cup 95," *Journal of Applied Meteorology*, Vol. 36, No. 6, 1997, pp. 711–720. https://doi.org/10.1175/1520-0450-36.6.711

[13] Ellenrieder, T. J., "The Modelling and Validation of the Vertical Dynamics of a Hot Air Balloon," *Journal of Aerospace Engineering*, Vol. 213, No. 1, 1999, pp. 57–62. https://doi.org/10.1243/0954410991532846

[14] Dai, Q., Fang, X., Li, X., and Tian, L., "Performance Simulation of High Altitude Scientific Balloons," *Advances in Space Research*, Vol. 49, No. 6, 2012, pp. 1045–1052. https://doi.org/10.1016/j.asr.2011.12.026

[15] Yajima, N., Imamura, T., Izutsu, N., and Abe, T., "Engineering Fundamentals of Balloons," *Scientific Ballooning*, Springer, New York, 2009, pp. 15–75. https://doi.org/10.1007/978-0-387-09727-5_2

[16] Saleh, S., and He, W., "Ascending Performance Analysis for High Altitude Zero Pressure Balloon," *Advances in Space Research*, Vol. 59, No. 8, 2017, pp. 2158–2172. https://doi.org/10.1016/j.asr.2017.01.040

Downloaded by Karina Bustillo on September 25, 2020 | http://arc.aiaa.org | DOI: 10.2514/1.C035890